

FIG. 6: AF theory predictions of disordered mode diffusivities for LJ argon alloy and amorphous phases. The thermal conductivity of the amorphous phase is well-described by a mode-independent diffusivity D_{HS} [Eq. (18)]. The system size for the alloy is $N_0 = 10$ (6,912 atoms), and the amorphous phase has 6,912 atoms.

In this section, in anticipation of the thermal conductivity predictions in Section IV, we discuss two possible sources of error in the VC-predicted mode properties. For disordered systems, it is generally only possible to assign a unique lifetime and group velocity to vibrational modes in the low-frequency, propagating limit.^{33,80} The mode diffusivity is the fundamental transport property.^{12,32,33}

We believe that the VC-predicted group velocities, particularly for $v_{g,n}(\vec{v}) \approx 0$, are an underprediction of the velocity scale required to evaluate Eq. (16). This statement is supported by the AF-theory diffusivities plotted in Fig. 6, which are finite for the LJ alloy at a concentration of 0.5. While the diffusivity from Eq. (16) can be zero because of the VC-predicted group velocities, this result is not consistent with the AF theory predictions.

The VC-NMD and Gamma-NMD predicted lifetimes are generally larger than the IR limit for LJ argon and its alloys (see Fig. 4). The constant lifetime observed at the highest frequencies for both VC-NMD (except at $c = 0.5$) and Gamma-NMD is consistent with the plateau of mode diffusivity at high frequency predicted for a model disordered lattice.⁷⁰ VC-ALD predicts essentially monotonically decreasing lifetimes with increasing frequency for the LJ argon alloys [Fig. 5(a)] with many falling below the IR limit. Because VC-NMD and VC-ALD use the same values for $v_{g,n}(\vec{v})$, the mode diffusivities will therefore be underpredicted for VC-ALD compared to VC-NMD for the LJ argon alloys.

IV. THERMAL CONDUCTIVITY PREDICTIONS

The thermal conductivities of the LJ systems can now be predicted from Eq. (1) using the

vibrational mode properties from VC-NMD and VC-ALD. Given the discussion regarding the VC-predicted mode properties in Section III E, we also predict thermal conductivity using the equilibrium MD-based GK method, which is a top-down method that does not make any approximations about the nature of the vibrational modes. Thermal conductivities predicted by the GK method naturally capture all scattering mechanisms.^{41,42,81} The heat current was computed every ten time steps from the same atomic trajectories (positions and velocities) used for the VC-NMD and Gamma-NMD calculations. The thermal conductivity is determined from the maximum of the integral of the heat current autocorrelation function.

The thermal conductivities predicted by VC-NMD, VC-ALD, and GK are system size-dependent [i.e., $k = k(N_0)$] for all lattices and methods except perfect LJ argon from GK. To predict a bulk thermal conductivity, k_{bulk} , a linear extrapolation procedure is used, whereby

$$\frac{k(N_0)}{k_{\text{bulk}}} = 1 - \frac{c_0}{N_0}, \quad \text{or } k_{\text{bulk}}? \text{ adjust } F_{37.9} \text{ axes labels} \quad (21)$$

where c_0 is a constant.¹⁸ The thermal conductivity is predicted for varying system sizes and the bulk thermal conductivity is obtained by fitting Eq. (21) ^{to the data}. For VC-NMD and VC-ALD, the validity of Eq. (21) requires that the low-frequency modes be dominated by phonon-phonon scattering (i.e., $\tau \propto \omega^{-2}$) and follow the Debye approximation with respect to the group velocity and DOS.^{18,19} For the LJ argon alloys, this requirement is satisfied for modest system sizes (for $N_0 = 6$ to 12) so that both VC-NMD and VC-ALD ^{thermal conductivity} predictions can be extrapolated to a bulk value.

Bulk thermal conductivity predictions for the LJ argon alloys using VC-NMD, VC-ALD, and GK are tabulated in Table I and plotted in Fig. 7. Also plotted in Fig. 7 is the ^{HS} ~~high-seatter~~ thermal conductivity prediction k_{HS} [Eq. (3)]. The thermal conductivity predicted for the LJ amorphous phase by GK is ~~0.17 W/m-K~~^{0.17 W/m-K}⁸² which is in good agreement with k_{HS} ~~(0.16 W/m-K)~~ ^{for the perfect crystal} using the VC predicted sound speed at a concentration of 0. The predicted thermal conductivities of the LJ argon alloys at high concentration are ~~only~~ ^a ~~several factors~~ ^{at - b -} larger than k_{HS} . While agreement between the three methods is found for the perfect crystal, VC-NMD and VC-ALD underpredict the alloy thermal conductivities compared to GK. The underprediction is modest for VC-NMD, where k_{NMD} is ~~about~~ ^{about} 80% of k_{GK} or greater for all concentrations. The VC-ALD method significantly underpredicts the thermal conductivity of the LJ argon alloys. The largest deviation is at a concentration of 0.05, where $k_{\text{VC-ALD}}$ is 56% of k_{GK} .

In Section IIID, we argued for the existence of a minimum mode ~~thermal~~ diffusivity, D_{HS} [Eq. (18)]. As shown in Fig. 5(b), the diffusivities of many high-frequency modes in the LJ alloys, predicted by both VC-NMD and VC-ALD, fall below this limit. Based on this observation, we propose that any diffusivity below the limit be set to D_{HS} for thermal conductivity prediction. The results of this adjustment, referred to as VC-NMD* and VC-ALD*, are plotted in Fig. 7 and included in Table I. The adjusted thermal conductivities predicted by VC-NMD* are now within ~~(at most)~~ ^{prediction} 10% of the GK value for all concentrations, which is within the ^{prediction} uncertainties. Combined with D_{HS} , we believe that the VC-NMD

predicted ~~thermal~~ diffusivities are good representations for the explicitly-disordered modes present in the MD simulation. ⁽³⁾ Another possible adjustment, D_{IR} [Eq. (19)], results in ~~an overprediction for LJ argon alloy at a concentration of 0.05, $k_{VC-NMD}, D_{IR} = 0.94 \pm 0.09$ W/m-K, compared to GK.~~ ^{athermal conductivity of 0.94 to 0.96 W/m-K for the} ^{well above k} ^{we also note that} ^{that} The thermal conductivity of the amorphous phase is well-modeled by a mode-independent diffusivity D_{HS} , while D_{IR} overpredicts for all modes in the amorphous phase (see Fig. 6). Thus, we believe D_{HS} is the more appropriate HS limit. ✓


By applying the HS limit adjustment VC-ALD*, the thermal conductivities are brought into marginally better agreement with the GK values, worst for a concentration of 0.05, where k_{VC-ALD^*} is 65% of k_{GK} . As seen in Fig. 5(b), the VC-ALD method fails to accurately predict the high-frequency mode diffusivities for LJ argon alloys. Since the group velocities are the same for VC-NMD and VC-ALD, the underprediction of the high-frequency diffusivities is due to the underprediction of the high-frequency mode lifetimes from VC-ALD compared to VC-NMD. We know ^{that} the VC-NMD predicted lifetimes are more ~~accurate~~ accurate values due to their agreement with Gamma-NMD (Fig. 4).

The thermal conductivity of LJ argon and its alloys ^{has important contributions from} ~~are dominated by~~ high-frequency modes. The thermal conductivity spectrum, defined as the contribution to thermal conductivity ^{of modes} at a given frequency, is plotted in Fig. 5(c) for VC-NMD and VC-ALD. VC-ALD underpredicts the high-frequency diffusivities compared to VC-NMD, ^{which} ~~This lead~~ ^s to an underprediction of the high-frequency thermal conductivity spectrum compared to VC-NMD. This result can be traced back to an underprediction of the high-frequency lifetimes compared to VC-NMD and Gamma-NMD [Fig. 5(a)].

For the perfect crystal and the alloy with a concentration of 0.05.

TABLE I: Thermal conductivity predictions using the VC-NMD, VC-ALD, and GK methods. For LJ argon alloys, the bulk extrapolation is used for all three methods. For SW silicon alloys, only VC-ALD and GK can be used to extrapolate a bulk thermal conductivity (see Section IV). For VC-NMD and GK, the uncertainties are estimated by omitting independent simulations from the ensemble averaging (see Section II C). For VC-ALD, the uncertainties are estimated by omitting extrapolation points used for Eq. (21).

c	VC-NMD	VC-ALD	VC-NMD*	VC-ALD*	GK	
LJ						
0.00	3.3 ± 0.1	3.4 ± 0.1			3.3 ± 0.1	
0.05	0.76 ± 0.07	0.45 ± 0.02	0.80 ± 0.1	0.52 ± 0.05	0.80 ± 0.07	
0.15	0.36 ± 0.04	0.24 ± 0.01	0.45 ± 0.05	0.33 ± 0.07	0.46 ± 0.07	
0.50	0.31 ± 0.04	0.23 ± 0.01	0.35 ± 0.05	0.31 ± 0.07	0.38 ± 0.07	
SW						
0.00		480 ± 20			520 ± 30	
0.05		24 ± 2		24 ± 2	20 ± 2	
0.15		12 ± 1		12 ± 1	9.9 ± 0.9	
0.50		11 ± 1		11 ± 1	9.3 ± 0.9	



 put GK first

V. SW SILICON

The failure of VC-ALD to predict the thermal conductivities of the LJ alloys is due to an underprediction of the high-frequency mode lifetimes, which dominate the thermal conductivity [see Sections III D and IV, Figs. 5(a) and 5(c)]. To provide a contrast, we now predict the mode properties and thermal conductivity for bulk and alloyed SW silicon, where it is known that low-frequency modes dominate the thermal conductivity.^{54,83} The lifetimes for the perfect crystal and an alloy concentration of 0.5 predicted by VC-NMD and VC-ALD are plotted in Fig. 8(a). The VC-NMD predicted lifetimes are generally larger than the IR limit for SW silicon alloys, similar to the VC-NMD predictions for the LJ argon alloys (Fig. 4). Unlike the LJ argon alloys, the VC-NMD and VC-ALD predicted lifetimes agree over most of the frequency spectrum, except at the highest frequencies, where VC-ALD underpredicts VC-NMD and falls below the IR limit. The high-frequency plateau of the VC-NMD predicted lifetimes for LJ argon (Fig. 4) is not seen for SW silicon. As seen in Figs. 5(b) and 8(b), VC-NMD and VC-ALD both predict a significant number of modes with $D_{ph}^{(v)}$ less than D_{HS} for both the LJ argon and SW silicon alloys.

The thermal conductivity spectrum for SW silicon alloy with a concentration of 0.5 is plotted in Fig. 8(c). For SW silicon alloy, the thermal conductivity is dominated by low-frequency modes, so that large system-sizes are needed to satisfy the extrapolation requirements and only GK and VC-ALD can be used to predict a bulk value $\kappa(N_0 \leq 42)$, similar to the converged system-sizes in Ref. [53]. This system-size requirement highlights the efficiency of the VC-ALD method, which is necessary when computationally expensive DFT calculations are used.^{8,15,17,19,84,85} SW silicon bulk thermal conductivity predictions for VC-ALD and GK are shown in Table I and plotted in Fig. 9. The thermal conductivities predicted for SW silicon alloys by VC-ALD are overpredicted by 20% compared to GK, in contrast to VC-ALD underpredicting for LJ argon alloys.⁸⁶

The predicted thermal conductivities for the SW silicon alloys at all concentrations are over an order of magnitude larger than the HS prediction, κ_{HS} . Because the thermal transport in SW silicon is dominated by low-frequency modes, the HS adjustment VC-ALD* is within one percent compared to the unadjusted VC-ALD. While higher-order interactions in the Tamura theory may be responsible for the discrepancy of the lifetimes predicted by VC-NMD and VC-ALD in SW silicon at the highest frequencies, this effect is not important

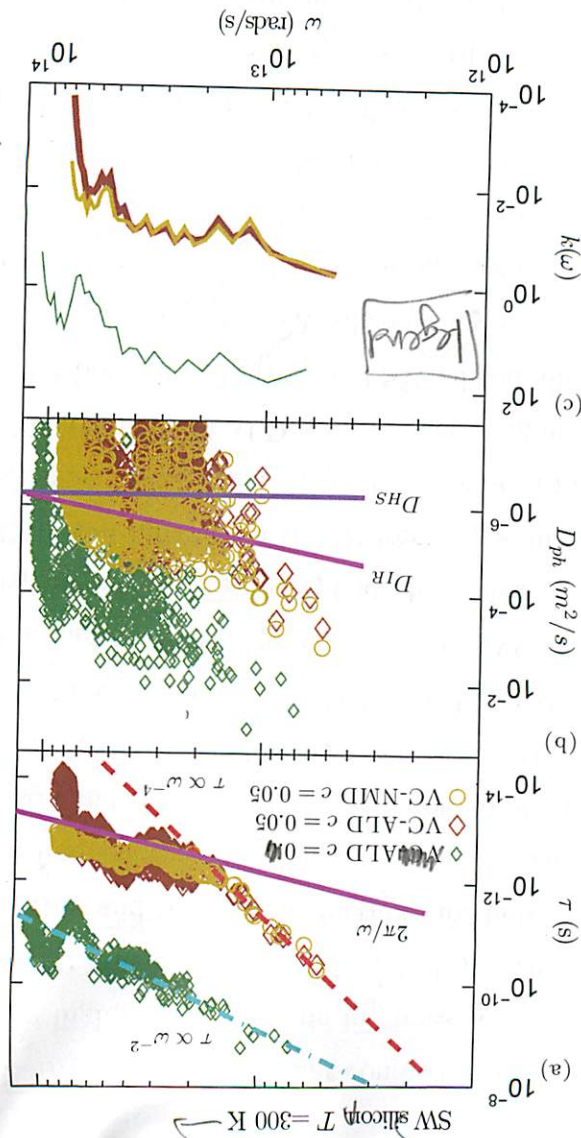
[53] 8/10/17

make an important contribution to

Standard application of the

frequency range where the Tamura theory is valid.
 to the overall thermal transport. We believe that VC-AID predicts accurate thermal con-
 ductivities for SW silicon because it is a low-frequency dominated material, which is the
 frequency spectrum, which is peaked at low frequency, in contrast to LJ argon (Fig. 5).

FIG. 8: (a) predicted lifetimes for VC modes using VC-NMD and VC-AID for SW silicon. (b)
 predicted VC mode diffusivities, compared to the AF,HS limit. (c) the thermal conductivity



[also for τ for ω]

units wt τ (s)

and τ (s)

write a
 better
 caption
 for
 this
 plot

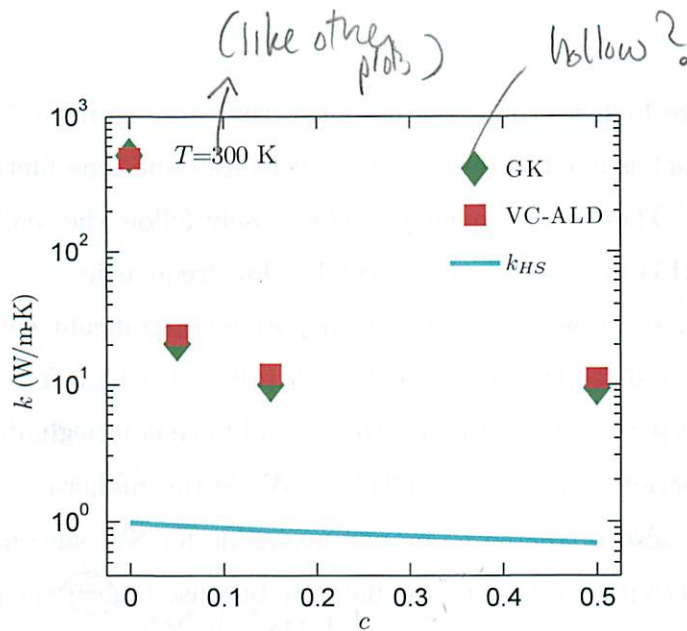


FIG. 9: Thermal conductivity predictions for SW silicon alloys at a temperature of 300 K using the VC-ALD and GK methods. The high-scatter thermal conductivity prediction k_{HS} is also plotted. The adjusted VC-ALD* is not shown since it differs by only one percent compared to VC-ALD.

VI. SUMMARY

In this study, we investigated the use of the VC approximation for predicting the vibrational mode properties and thermal conductivity of LJ argon and SW silicon alloys by a detailed comparison of the NMD, VC-ALD, and GK methods. By using computationally-inexpensive empirical potentials we self-consistently studied the effects of disorder both explicitly (Sections III A, III B, III C 1, III D, and V) and as a perturbation (Sections III C 2 and V). By spanning a range of disorder, the limits of the perturbative models were examined. A breakdown of the VC-ALD method was identified for LJ argon alloys by a comparison with the NMD method in Section III C 2 and a correction was suggested in Section III D. The mode properties and thermal conductivity of the SW silicon alloys were predicted and in Section V and provided a contrast to the LJ argon alloys, which have different thermal conductivity spectra.

The results for the SW silicon and LJ argon alloys suggest that modeling of thermal transport in ordered and disordered lattices can be separated into two broad groups: low-frequency dominated and full-spectrum materials. Materials dominated by low-frequency

modes tend to have high thermal conductivities that are significantly larger than the HS limit [Eq. (3)], which is due to the large group velocities and long lifetimes of low-frequency modes.^{8-10,15,38-40,87} These low-frequency modes closely follow the scalings predicted by the perturbative VC-ALD models, which are valid at low-frequencies.

LJ argon is a material whose thermal transport has significant contribution from high-frequency modes, even for the bulk [see Fig. 5 (c)]. This high-frequency range is where we predict that the perturbative Tamura theory will have non-negligible contributions from higher-order interactions (see Section III C 2). While the higher-order interactions in the Tamura theory are also predicted to be non-negligible for SW silicon, this does not affect the thermal conductivity predictions significantly because high-frequency modes are not important to thermal transport. The ~~unimportance~~ ^{negligible contribution} of high-frequency modes is also true for the thermal conductivity spectrum of SiGe alloys from theoretical predictions^{10,14,15} and experimental measurements where the thermal conductivity exceeds the HS limit by more than an order of magnitude at room temperature for all compositions.^{1,39,40,87}

The VC-ALD method provides a computationally inexpensive framework, which is essential when using *ab initio* methods for predicting thermal conductivity.^{8,14-21} Based on our results, we believe ~~that~~ ^{that} the Tamura theory breaks down for mode ~~thermal~~ diffusivities predicted to be below the HS limit, D_{HS} [Eq. (18)]. This breakdown may be true for the high-frequency modes of any disordered lattice⁷⁰ and the high-scatter limit D_{HS} should be considered whenever the perturbative VC-ALD method is used. Although the HS limit of ~~thermal~~ diffusivity is usually interpreted as a minimum mean free path,^{1,70,88,89} we find that this concept is not necessary for interpreting the results of this work. In a disordered lattice, the fundamental quantity ^{is the mode lifetime} ~~is~~ ^{and diffusivity} ~~and~~ the VC predicted group velocity is an approximation. Expressed together as ^a ~~diffusivity~~, the VC-predicted mode properties can be used to compare with thermal transport in the explicitly disordered lattice. ^{needed?}

Acknowledgments

This work was supported by AFOSR award FA95501010098 and by a grant of computer time from the DOD High Performance Computing Modernization Program at the US Army Engineer Research and Development Center. We thank Davide Donadio, Jivtesh Garg, Asad Hasan, Craig Maloney, and Zhiting Tian for helpful discussions.

Appendix A: NMD using Non-Exact Normal Modes

For a normal mode of the lattice supercell used for the MD simulations (i.e., a Gamma mode), the total energy autocorrelation is an exponential function with a decay time $\tau(\nu)$ and the kinetic energy autocorrelation is a exponentially-damped sinusoidal oscillation with frequency $2\omega(\nu)$. (cite AHRT) When projecting onto the VC normal modes from MD simulations of the explicitly disordered lattice supercells, the energy autocorrelation functions do not always follow the simple functional forms, as shown in Fig. 10. By calculating the mode ^{kinetic} energy in the frequency-domain, Φ ,³¹ artifacts such as multiple peaks are observed. ^(see main plot) for high concentrations, $c = 0.5$, Fig. 10.

These artifacts are not surprising given two considerations: (i) the MD simulations contain explicit disorder ^{that} influences the atomic trajectories, and (ii) the VC ~~normal~~ modes are not the exact normal modes of the explicitly-disordered lattice supercells. An effective lifetime can be predicted using Eq. (11) because the VC total mode energy autocorrelations still decay to zero in a finite time. This results is to be expected given that the atomic trajectories contain information about the lattice energy, which from general statistical physics principles will have exponential relaxation behavior in an equilibrium ensemble.⁹⁰⁻⁹²

For two modes in
the alloy with $c=0.5$

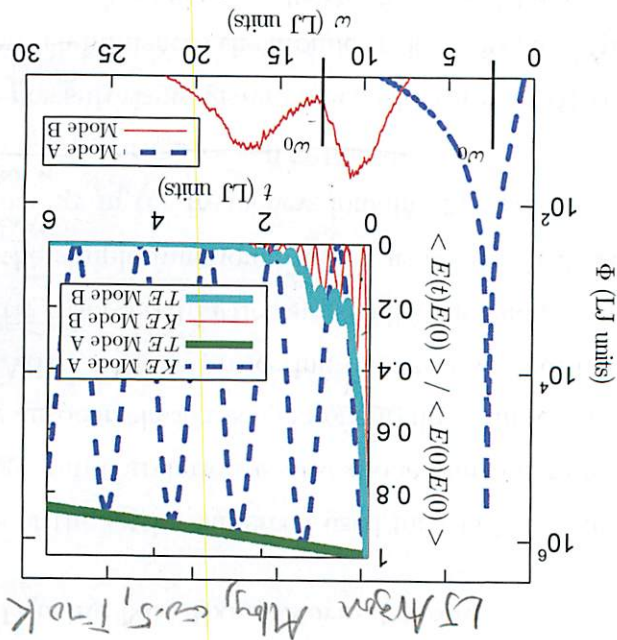
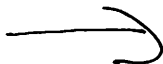


FIG. 10: The normal mode kinetic energy Φ of two modes (A and B) at wavevector $[0.25\ 0\ 0]$ calculated using VC-NMD for a mass disordered LJ FCC supercell ($N_0 = 8$ and $c = 0.5$) is shown in the main figure. The VC dispersion-predicted peaks are labeled by ω_0 . The inset shows the same mode's energy [kinetic (KE) and total (TE)] autocorrelation functions. Note the additional oscillation effects in the KE and TE autocorrelation functions for Mode B which are due to the double peaks in Φ . A mode lifetime can be extracted unambiguously using the integral of the TE autocorrelation function (Section III C 1).

- ³⁵ P. G. Klemens, Proceedings of the Physical Society. Section A **70**, 833 (1957), URL <http://stacks.iop.org/0370-1298/70/i=11/a=407>.
- ³⁶ J. Callaway, Physical Review **113**, 1046 (1959).
- ³⁷ D. C. Mattis, Phys. Rev. **107**, 17361736 (1957), URL <http://link.aps.org/doi/10.1103/PhysRev.107.1736.3>.
- ³⁸ W. A. Kamitakahara and B. N. Brockhouse, Phys. Rev. B **10**, 12001212 (1974), URL <http://link.aps.org/doi/10.1103/PhysRevB.10.1200>.
- ³⁹ D. G. Cahill and F. Watanabe, Phys. Rev. B **70**, 235322 (2004), URL <http://link.aps.org/doi/10.1103/PhysRevB.70.235322>.
- ⁴⁰ D. G. Cahill, F. Watanabe, A. Rockett, and C. B. Vining, Phys. Rev. B **71**, 235202 (2005), URL <http://link.aps.org/doi/10.1103/PhysRevB.71.235202>.
- ⁴¹ A. Skye and P. K. Schelling, Journal of Applied Physics **103**, 113524 (2008), URL <http://link.aip.org/link/?JAP/103/113524/1>.
- ⁴² E. S. Landry, M. I. Hussein, and A. J. H. McGaughey, Physical Review B **77**, 184302 (2008).
- ⁴³ E. S. Landry and A. J. H. McGaughey, Physical Review B **80**, 165304 (2009).
- ⁴⁴ Z. Tian, K. Esfarjani, and G. Chen, Phys. Rev. B **86**, 235304 (2012), URL <http://link.aps.org/doi/10.1103/PhysRevB.86.235304>.
- ⁴⁵ J. E. Turney, PhD thesis, Carnegie Mellon University, Pittsburgh, PA (2009).
- ⁴⁶ I. Kudman, Journal of Materials Science **7**, 1027 (1972), ISSN 0022-2461, URL <http://dx.doi.org/10.1007/BF00550066>.
- ⁴⁷ Y. Pei, X. Shi, A. LaLonde, H. Wang, L. Chen, and G. J. Snyder, Nature **473**, 66 (2011), ISSN 0028-0836, URL <http://dx.doi.org/10.1038/nature09996>.
- ⁴⁸ Y. K. Koh, C. J. Vineis, S. D. Calawa, M. P. Walsh, and D. G. Cahill, Applied Physics Letters **94**, 153101 (2009), URL <http://link.aip.org/link/?APL/94/153101/1>.
- ⁴⁹ K. Momma and F. Izumi, Journal of Applied Crystallography **41**, 653658 (2008), URL <http://dx.doi.org/10.1107/S0021889808012016>.
- ⁵⁰ A. J. H. McGaughey, PhD thesis, University of Michigan, Ann Arbor, MI (2004).
- ⁵¹ S. Plimpton, Journal of Computational Physics **117**, 1 (1995), ISSN 0021-9991, URL <http://www.sciencedirect.com/science/article/pii/S002199918571039X>.
- ⁵² J. V. Goicochea, M. Madrid, and C. H. Amon, Journal of Heat Transfer **132**, 012401 (2010).
- ⁵³ Y. He, I. Savic, D. Donadio, and G. Galli, Phys. Chem. Chem. Phys. pp. – (2012), URL

<http://dx.doi.org/10.1039/C2CP42394D>.

- ⁵⁴ D. P. Sellan, J. E. Turney, A. J. H. McGaughey, and C. H. Amon, *Journal of Applied Physics* **108**, 113524 (2010).
- ⁵⁵ J. D. Gale and A. L. Rohl, *Molecular Simulation* **29**, 291 (2003).
- ⁵⁶ A. M. Bouchard, R. Biswas, W. A. Kamitakahara, G. S. Grest, and C. M. Soukoulis, *Phys. Rev. B* **38**, 1049910506 (1988), URL <http://link.aps.org/doi/10.1103/PhysRevB.38.10499>.
- ⁵⁷ J. C. Duda, T. S. English, D. A. Jordan, P. M. Norris, and W. A. Soffa, *Journal of Physics: Condensed Matter* **23**, 205401 (2011), URL <http://stacks.iop.org/0953-8984/23/i=20/a=205401>.
- ⁵⁸ Q.-J. Chu and Z.-Q. Zhang, *Phys. Rev. B* **39**, 71207131 (1989), URL <http://link.aps.org/doi/10.1103/PhysRevB.39.7120>.
- ⁵⁹ A. J. H. McGaughey and M. Kaviani, in *Advances in Heat Transfer, Volume 39*, edited by G. A. Greene, Y. I. Cho, J. P. Hartnett, and A. Bar-Cohen (Elsevier, 2006), p. 169255.
- ⁶⁰ Y. He, D. Donadio, J.-H. Lee, J. C. Grossman, and G. Galli, *ACS Nano* **5**, 1839\961844 (2011).
- ⁶¹ Y. He, D. Donadio, and G. Galli, *Applied Physics Letters* **98**, 144101 (2011).
- ⁶² D. Donadio and G. Galli, *Phys. Rev. Lett.* **102**, 195901 (2009).
- ⁶³ S. Volz and G. Chen, *Physical Review B* **61**, 26512656 (2000).
- ⁶⁴ N. L. Green, D. Kaya, C. E. Maloney, and M. F. Islam, *Physical Review E* **83**, 051404 (2011), URL <http://link.aps.org/doi/10.1103/PhysRevE.83.051404>.
- ⁶⁵  ~~we, f_{nl} (2013),~~ ^{due to the} for a finite-size system, the delta function in Eq. \eqref{EQ:SLT} is broadened using a Lorentzian function with a full-width at half maximum set to $20_{\text{mega,avg}}$, where mega,avg is the average frequency spacing.\cite{feldman-thermal-1993}.
- ⁶⁶ A. J. C. Ladd, B. Moran, and W. G. Hoover, *Physical Review B* **34**, 50585064 (1986).
- ⁶⁷ J. E. Turney, E. S. Landry, A. J. H. McGaughey, and C. H. Amon, *Physical Review B* **79**, 064301 (2009).
- ⁶⁸ M. T. Dove, *Introduction to Lattice Dynamics* (Cambridge, Cambridge, 1993).
- ⁶⁹ A. A. Maradudin and A. E. Fein, *Physical Review* **128**, 25892608 (1962).
- ⁷⁰ P. Sheng and M. Zhou, *Science* **253**, 539542 (1991), URL <http://www.sciencemag.org/content/253/5019/539.abstract>.
- ⁷¹ S. N. Taraskin and S. R. Elliott, *Philosophical Magazine Part B* **79**, 17471754 (1999), URL <http://www.tandfonline.com/doi/abs/10.1080/13642819908223057>.

- ⁷² D. J. Ecsedy and P. G. Klemens, Phys. Rev. B **15**, 59575962 (1977), URL <http://link.aps.org/doi/10.1103/PhysRevB.15.5957>.
- ⁷³ ~~vc, fn2~~ (2013), To perform the calculation of Eq. \eqref{EQ:taud_dos}, it is necessary to broaden the DOS using using a Lorentzian function. \cite{tamura_isotope_1983} For all calculations using Eq. \eqref{EQ:taud_dos}, the Lorentzian was broadened using a value of mega_{avg} . The results do not differ significantly if this broadening value is varied manually or by increasing the system size. *? necessary?*
- ⁷⁴ ~~vc, fn3~~ (2013), The CP model and HS limit thermal conductivity predictions differ by a ~~constant factor of~~ approximately 20% because the CP model assumes a mode-specific lifetime $\tau = 2\pi/\text{mega}$. \cite{cahill_lattice_1988}.
- ⁷⁵ S. Shenogin, A. Bodapati, P. Keflikli, and A. J. H. McGaughey, Journal of Applied Physics **105**, 034906 (2009), URL <http://link.aip.org/link/?JAP/105/034906/1>.
- ⁷⁶ P. Sheng, *Introduction to Wave Scattering: Localization and Mesoscopic Phenomena* (Springer, 2006), ISBN 9783540291565.
- ⁷⁷ V. Vitelli, N. Xu, M. Wyart, A. J. Liu, and S. R. Nagel, Phys. Rev. E **81**, 021301 (2010), URL <http://link.aps.org/doi/10.1103/PhysRevE.81.021301>.
- ⁷⁸ ~~vc, fn4~~ (2013), For a finite system, the AF theory requires a frequency broadening to predict the mode-specific thermal diffusivities. \cite{allen_thermal_1993} We ^{broaden using a} use a Lorentzian broadening ^{Function} with a width of mega_{avg} .
- ⁷⁹ ~~vc, fn5~~ (2013), ^{with} for the disordered lattices studied in this work ~~for~~ $\text{sc} \leq 0.15$, the predicted AF is strongly system size dependent, indicating this diverging behavior. For LJ argon alloys at $\text{sc}=0.5$, the divergence with system size is small for the range of system size studied ($N_0=4$ to $N_0=12$), where $k_{\text{AF}}/k_{\text{GK}} = 0.93$ for $N_0=12$ because the finite system size limits the diffusivities of the lowest frequencies.
- ⁸⁰ N. Xu, V. Vitelli, M. Wyart, A. J. Liu, and S. R. Nagel, Phys. Rev. Lett. **102**, 038001 (2009), URL <http://link.aps.org/doi/10.1103/PhysRevLett.102.038001>.
- ⁸¹ E. S. Landry and A. J. H. McGaughey, Physical Review B **79**, 075316 (2009).
- ⁸² ~~vc, fn6~~ (2013), The AF theory predicted thermal conductivity of the amorphous LJ argon phase is $k_{\text{AF}}=0.14$ W/m-K using a broadening of mega_{avg} . The thermal conductivity is proportional to the broadening used, but to remain consistent we do not adjust to bring AF into better agreement with GK. *Is this comment really needed?*

- ⁸³ D. P. Sellan, E. S. Landry, J. E. Turney, A. J. H. McGaughey, and C. H. Amon, Physical Review B **81**, 214305 (2010), URL <http://link.aps.org/doi/10.1103/PhysRevB.81.214305>.
- ⁸⁴ K. Esfarjani and H. T. Stokes, Physical Review B **77**, 144112 (2008).
- ⁸⁵ L. Chaput, A. Togo, I. Tanaka, and G. Hug, Phys. Rev. B **84**, 094302 (2011), URL <http://link.aps.org/doi/10.1103/PhysRevB.84.094302>.
- ⁸⁶ ~~we, for (2013)~~, The overprediction of thermal conductivity by VC-ALD compared to GK may be related to the role of disorder in the ALD calculation. \citegarg_role_2011 By including disorder in the ALD calculation explicitly, Garg et al found an overprediction of VC-ALD compared to experiment by a factor of two. The overprediction by VC-ALD that we observe is not as drastic.
- ⁸⁷ R. Cheaito, J. C. Duda, T. E. Beechem, K. Hattar, J. F. Ihlefeld, D. L. Medlin, M. A. Rodriguez, M. J. Campion, E. S. Piekos, and P. E. Hopkins, Phys. Rev. Lett. **109**, 195901 (2012), URL <http://link.aps.org/doi/10.1103/PhysRevLett.109.195901>.
- ⁸⁸ C. Kittel, Physical Review **75**, 974 (1949).
- ⁸⁹ J. E. Graebner, B. Golding, and L. C. Allen, Phys. Rev. B **34**, 56965701 (1986), URL <http://link.aps.org/doi/10.1103/PhysRevB.34.5696>.
- ⁹⁰ G. P. Srivastava, *The Physics of Phonons* (Adam Hilger, Bristol, 1990).
- ⁹¹ L. Landau, E. Lifshitz, and L. Pitaevskii, *Statistical Physics, Part 2 : Volume 9*, Pt 2 (Elsevier Science & Technology Books, 1980), ISBN 9780750626361, URL <http://books.google.com/books?id=NaB7oAkon9MC>.
- ⁹² A. Rajabpour and S. Volz, Journal of Applied Physics **108**, 094324 (2010), URL <http://link.aip.org/link/?JAP/108/094324/1>.

This
 discussion
 needs to
 be in
 the
 main
 text -
 Sections
 II B
 and
 II